Inelastic neutron scattering determination of phonon dispersion curves in the molecular crystal *sym*-$C_6F_3Cl_3$

M. T. Dove
Department of Earth Sciences, University of Cambridge CB2 3EQ, United Kingdom

B. M. Powell
Atomic Energy of Canada Limited, Chalk River Nuclear Laboratories, Chalk River, Ontario K0J 1J0, Canada

G. S. Pawley
Department of Physics, University of Edinburgh, Kings Buildings, Edinburgh EH9 3JZ, United Kingdom

S. L. Chaplot
Nuclear Physics Division, Bhabha Atomic Research Centre, Bombay 400 085, India

A. Mierzejewski
Technical University of Wrocław, Wrocław, Poland

(Received 26 July 1988; accepted 18 October 1988)

Phonon dispersion curves have been obtained along the Δ, Σ, and T directions in a single crystal of *sym*-$C_6F_3Cl_3$ at 5 K by inelastic neutron scattering measurements. These have been interpreted within the framework of rigid-molecule lattice dynamics. A model intermolecular potential reproduces the overall behavior, but there remains scope for improvement in the model. Other models based on transferable potentials are found to be less satisfactory.

I. INTRODUCTION

The study of phonons in molecular crystals has expanded greatly in the last few years. One reason for this is that measurements of the phonon dispersion relations provide information about intermolecular potentials; in particular they are a test of the extent to which features of intermolecular potentials are universal and so directly transferable between different molecules. An example of such "universality" is the development of sets of transferable atom–atom pair potentials. A second reason is that the detailed excitation spectrum provides information about the nature and mechanism of structural transitions in molecular solids, a field of increasing interest.

The most detailed investigations of atom–atom potentials have been made for carbon and hydrogen.[1] Consequently, many of the phonon measurements have been made on simple, aromatic hydrocarbons to assess the reliability of these model potentials. For example, the measured intermolecular mode frequencies in *d*-benzene[2] agree reasonably well with those calculated from model potentials. Most of these measurements were confined to symmetry points, with few data points inside the Brillouin zone. An alternative set of potential parameters was subsequently found to fit the data equally well. These parameters appeared unphysical but recent work[3] suggests that they represent a very successful "effective" model for benzene. This ambiguity does not occur in analysis of the detailed phonon measurements in *d*-naphthalene[4] and *d*-anthracene[5] where good agreement is found between the measured and calculated intermolecular frequencies. Initially, electrostatic interactions were not included in these potentials, but despite their success, it was recognized that electrostatic forces must play a role in the aromatic hydrocarbons.[1] The inclusion of a quadrupole moment in the calculation for naphthalene led to improved agreement with the experimental frequencies.[6]

It is desirable that the range of molecular crystals for which extensive dispersion curves have been measured should be increased and that molecules containing atoms other than carbon and hydrogen should be investigated. In particular, recent potentials for nitrogen and the halogens should be tested.[7] Relatively few measurements have been made on molecules containing these atoms; examples are given in Ref. 8. The molecular crystal *sym*-trifluoro-trichloro-benzene, *sym*-$C_6F_3Cl_3$ is of interest in this context because it contains two different halogen atoms. The crystal structure of *sym*-$C_6F_3Cl_3$ is hexagonal (space group $P6_3/m$) with two planar molecules in the unit cell.[9] The molecules lie in the basal plane on sites with symmetry $\bar{6}$ and are stacked along the hexagonal axis. The crystal structure is shown in Fig. 1. The crystal structure of *sym*-$C_6F_3Cl_3$ is similar to that of *sym*-triazine (*sym*-$C_3N_3H_3$)[10] with regard to the parallel stacking of molecules. But, whereas the latter under-

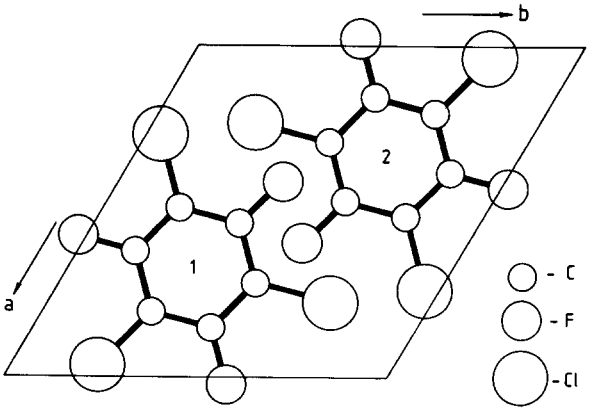

FIG. 1. The crystal structure of $C_6F_3Cl_3$ viewed down the hexagonal *c* axis. Molecule 1 is at height $c/4$, and molecule 2 is at height $3c/4$.

 0021-9606/89/031918-06$02.10

goes a phase transition at 198 K in which a molecular rotation out of the basal plane is coupled to a shear distortion of the unit cell,[11] the hexagonal structure of *sym*-$C_6F_3Cl_3$ is stable down to the lowest temperatures.[9] Interpretation of the phonon dispersion relation may lead to an understanding of this difference in behavior of these two similar molecular solids.

In the present paper we report coherent, inelastic neutron scattering measurements of the dispersion curves of intermolecular modes propagating along the Δ, Σ, and T directions in *sym*-$C_6F_3Cl_3$ at 5 K. In the next section the details of the experimental measurements and of the initial calculations are given. The experimental results are discussed in Sec. III, while available model potentials are assessed in Sec. IV.

II. EXPERIMENTAL DETAILS AND MODEL CALCULATIONS

The measurements were made on two different single crystals of *sym*-$C_6F_3Cl_3$ with volumes of 7 and 1 cm^3, respectively, both grown in Edinburgh. The raw material was initially purified by zone refining, and the crystals were then grown from the melt. Three crystal orientations were used: (i) with **c*** and **a*** in the scattering plane, (ii) with the basal plane as the scattering plane, and (iii) with **c*** and a [110] direction in the scattering plane. The measurements were made on the C5 and L3 triple-axis spectrometers at the NRU reactor, Chalk River, at a temperature of 5 K. Monochromators used were Si(111) and Cu(111) and the corresponding analyzers were graphite (0002) and Si(111). The majority of measurements were made with an analyzing frequency of 3.5 THz and the spectrometer resolutions, defined as the width of the incoherent scattering from vanadium, were 0.24 and 0.19 THz, respectively.

Since *sym*-$C_6F_3Cl_3$ has two molecules in the hexagonal unit cell, 12 intermolecular vibrational modes exist, and for a general wave vector in the Brillouin zone there will be 12 independent intermolecular frequencies. The labeling of the points and directions in the zone are shown in Fig. 2. Symmetry reduces the number of independent frequencies for particular points and directions. Along **c*** (Δ) the modes can be classified into two groups with four doubly degenerate and four nondegenerate frequencies. The same classification occurs at both the $\Gamma(000)$ and $K(1/3\ 1/3\ 0)$ points. At the $A(0\ 0\ 1/2)$ point there are two modes of fourfold degeneracy and two modes with double degeneracy.

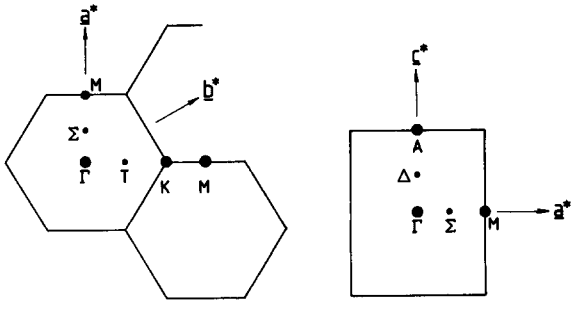

FIG. 2. (a) Plan of reciprocal space viewed down the **c*** direction, showing the Brillouin zone boundaries and the points of special symmetry. (b) Plan of reciprocal space viewed down the [1$\bar{2}$0] direction, showing the Brillouin zone boundaries and the points of special symmetry.

But even at these higher symmetry points the number of independent frequencies is sufficiently large that the inelastic neutron scattering measurements can be interpreted only with the help of precalculated one-phonon structure factors. These structure factors were calculated from a harmonic lattice dynamical model assuming the *sym*-$C_6F_3Cl_3$ molecule to be rigid.[12] This assumption is only justified if the lowest internal vibrational frequency is higher than the highest external lattice vibration. The lowest internal mode frequency is 3 THz in the gas phase and 3.54 THz in the solid phase,[13] and the highest lattice mode frequency as measured in this work is 2.86 THz [Fig. 3(b)]. The significant shift of the internal mode frequency between the gas and the solid phases suggests a strong coupling to the highest lattice mode. This could be treated by the method of Pawley and Cyvin,[14] but, for simplicity, we retain the rigid-molecule approximation. This assumption should be appropriate for most of the lattice modes of *sym*-$C_6F_3Cl_3$, but will not be as valid for the highest frequency lattice modes. The intermolecular potential was assumed to be a sum over pairwise atom–atom interactions of "six-exponential" form:

$$V=\frac{1}{2}\sum_{ij}\left[-\frac{A_{ij}}{r_{ij}^6}+B_{ij}\exp(-C_{ij}r_{ij})\right],$$

where r_{ij} is the interatomic separation between atoms i and j in different molecules and A_{ij}, B_{ij}, C_{ij} are the parameters specifying the potential between these atoms. Values for these parameters were derived by Chaplot[15] using the observed crystal structure at 5 K[9] and three lattice frequencies measured at 11 K by Raman scattering. They are given in Table I. The present calculations were performed using the equilibrium crystal structure at 5 K for the model. The equilibriated structure has lattice parameters $a=8.43$ Å, $c=5.81$ Å compared with observed values[9] of $a=8.44$ Å, $c=6.05$ Å. With this model for the intermolecular forces, the one-phonon structure factors were calculated and the peaks observed in the scattered neutron distributions were assigned to the appropriate mode on the basis of these structure factors. The precalculation of one-phonon structure factors from a lattice dynamical model is essential if inelastic neutron scattering data is to be successfully interpreted for crystals as complex as *sym*-$C_6F_3Cl_3$. This approach was used in the investigations of the hydrocarbons discussed above.[2,4–6]

TABLE I. Potential parameters from Chaplot (Ref. 15) used in our phonon calculations.

Atom pair	A(kcal Å^6 mol^{-1})	B(kcal mol^{-1})	C(Å^{-1})
C–C	387.87	42 000.0	3.532
C–F	351.64	42 000.0	3.804
C–Cl	829.82	42 000.0	3.297
F–F	307.64	42 000.0	4.121
F–Cl	775.75	42 000.0	3.532
Cl–Cl	1728.51	42 000.0	3.091

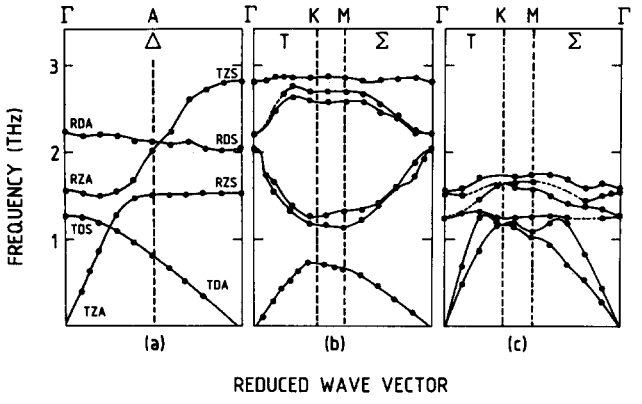

FIG. 3. Measured phonon frequencies of $C_6F_3Cl_3$ along the high symmetry directions. The measured frequencies are shown as filled circles, and the lines are given as guides to the eye. Broken lines are given for parts of a branch that were unobservable. The separate figures are for (a) phonons along **c*** with unfolding of the Brillouin zone (the labels refer to the modes at Γ); (b) phonons in the basal plane with out-of-plane atomic motions; (c) phonons in the basal plane with in-plane atomic motions.

III. EXPERIMENTAL RESULTS

A. Phonons along the c* (Δ) direction

Phonons propagating along **c*** can be uniquely characterized according to the nature of their eigenvectors. At Γ all modes are either pure translational or pure librational (rotational) while along Δ the two types of displacement are mixed, $\pi/2$ out-of-phase. Further, the molecular motion can be characterized according to the direction of the translational displacement or the axis of the librational displacement. Consequently, we classify the modes using a notation similar to that employed for CS_2 [16] with three letters describing each mode. The translational or librational character of the eigenvector is specified by *T* or *R*, respectively. Modes whose translational eigenvector is perpendicular to **c*** or whose axis of libration lies in the molecular plane are doubly degenerate and are designated by *D*. Modes whose translational eigenvector is along **c*** or whose axis of libration is parallel to **c*** are nondegenerate and are designated by *Z*. Finally, symmetric or antisymmetric displacements of the two molecules in the unit cell with respect to the inversion center are designated by *S* and *A*, respectively.

Using the precalculated one-phonon structure factors, most of the eight independent branches could be unambiguously identified by the inelastic neutron scattering measurements; the only uncertainties concerned the branches with very similar frequencies. The experimental dispersion curves are shown in Fig. 3(a) and the observed frequencies are given in Table II. The solid lines through the data points in Fig. 3 are a guide to the eye.

B. Phonons in the basal plane

In the basal plane, measurements were made for branches in both Σ [100] and *T* [110] directions. Except at the points Γ and *K* there are no degeneracies required by symmetry. Further, the eigenvectors of the 12 modes can be separated into only two classes; those with translational displacements along **c*** and a librational axis lying in the molecular plane (thus giving atomic motion along **c***) and those with translational displacements in the basal plane and the librational axis along the molecular threefold axis (the **c** axis, thus giving atomic motion parallel to the basal plane). All modes are of mixed translational–librational character and the displacements of the two molecules in the unit cell are not simply symmetric or antisymmetric with respect to the inversion center. At *K* the symmetry conditions are more stringent. At this point there are four doubly degenerate and four nondegenerate frequencies, and the modes are either symmetric or antisymmetric although still of mixed character.

It was not possible to identify all modes at all propagation vectors for these two basal plane directions. Because of the large number of distinct modes and the lower symmetry of these directions, interpretation of the experimental groups with the precalculated structure factors was less definitive than for the **c*** direction. Accordingly, there remains some ambiguity concerning the exact assignment of modes 4–6 for the branches in the basal plane with in-plane atomic motions. Because these modes have very similar frequencies, this uncertainty in mode assignment will not pose a significant problem when the data are used for the evaluation of model potentials (Sec. IV). The experimental dispersion curves for modes with out-of-plane and in-plane atomic motions are shown in Figs. 3(b) and 3(c), respectively, and the observed frequencies are given in Table III.

TABLE II. Measured phonon frequemcies (in THz) for modes with wave vectors along Δ. The notation used to describe the symmetry of the modes is described in the text. Estimated errors on the last significant figure of the frequencies are given in brackets. The dash indicates a measurement that could not be taken because of overlap of the phonon group with the tail of a Bragg peak. At the A point there is increased degeneracy.

Reduced wave vector	TZA	RZS	TZS	RZA	TDS	TDA	RDA	RDS
0.0 (Γ)	0.0	1.54(3)	2.80(3)	1.57(3)	1.26(2)	0.0	2.22(3)	2.04(4)
0.1	0.40(4)	1.53(3)	2.80(3)	1.53(3)	1.27(3)	···	2.16(4)	2.03(3)
0.2	0.88(2)	1.54(2)	2.70(3)	1.50(3)	1.19(3)	0.36(1)	2.21(2)	2.04(2)
0.3	1.28(2)	1.51(2)	2.60(2)	1.56(3)	1.10(3)	0.52(1)	2.19(2)	2.14(3)
0.4	1.49(2)	1.51(2)	2.22(2)	1.68(2)	0.98(2)	0.67(1)	2.12(4)	2.08(3)
0.5(A)	1.51(2)	1.51(2)	2.03(3)	2.03(3)	0.82(2)	0.82(2)	2.13(3)	2.13(3)

TABLE III. Measured phonon frequencies for modes propagating in the basal plane. Estimated errors on the last significant figures of the measurements are given in brackets. A dash indicates that a particular mode was not observed. Frequencies are given in THz.

A. Modes with out-of-plane atomic motions						
Wave vector	Mode 1	Mode 2	Mode 3	Mode 4	Mode 5	Mode 6
0.1,0,0	0.16(4)	1.72(3)	1.88(3)	2.22(3)	2.24(2)	2.85(3)
0.2,0,0	0.30(2)	1.60(3)	1.62(2)	2.38(3)	2.40(3)	2.84(3)
0.3,0,0	0.46(3)	1.40(3)	1.42(3)	2.45(2)	2.54(3)	2.82(4)
0.4,0,0	0.58(3)	1.22(2)	1.36(3)	2.57(3)	2.67(4)	2.81(4)
0.5,0,0 = 0.5,0.5,0	0.66(3)	1.14(3)	1.33(3)	2.58(3)	2.69(3)	2.84(3)
0.4,0.4,0	0.71(3)	1.18(4)	1.28(4)	2.58(4)	2.70(4)	2.86(4)
0.3,0.3,0	0.74(3)	1.20(4)	1.26(4)	2.59(4)	2.68(4)	2.84(4)
0.2,0.2,0	0.51(3)	1.34(4)	1.38(4)	2.63(4)	2.75(4)	2.85(4)
0.1,0.1,0	0.28(3)	1.56(4)	1.68(4)	2.46(4)	···	2.85(4)
B. Modes with in-plane atomic motions						
Wave vector	Mode 1	Mode 2	Mode 3	Mode 4	Mode 5	Mode 6
0.1,0,0	0.28(3)	0.44(3)	1.25(3)	1.34(4)	1.50(3)	1.63(3)
0.2,0,0	0.54(3)	0.84(4)	···	1.37(6)	1.44(4)	1.58(3)
0.3,0,0	0.72(4)	1.18(4)	1.25(4)	1.40(3)	···	1.68(4)
0.4,0,0	0.94(3)	1.19(3)	1.28(3)	1.50(4)	···	1.74(3)
0.5,0,0 = 0.5,0.5,0	1.04(3)	1.09(3)	1.27(3)	1.58(3)	1.66(3)	1.74(3)
0.4,0.4,0	1.14(3)	1.20(3)	1.26(4)	1.55(4)	1.66(3)	1.72(3)
0.3,0.3,0	1.16(3)	1.20(3)	1.27(4)	1.62(4)	···	···
0.2,0.2,0	0.90(2)	1.26(4)	1.33(4)	1.46(4)	···	1.70(3)
0.1,0.1,0	0.49(3)	0.70(4)	1.30(3)	···	1.52(3)	1.58(3)

C. Elastic constants

The slopes of the acoustic branches at small propagation vectors (i.e., long wavelengths) are the velocities of sound. From the measured values we can determine four of the five elastic constants of *sym*-$C_6F_3Cl_3$, i.e., C_{11}, C_{33}, C_{44}, and C_{66} [$= (1/2)(C_{11}-C_{12})$]. The values are given in Table IV.

IV. DISCUSSION

Most of the lattice mode frequencies lie well below the lowest frequency of the internal vibrations,[13] so that the rigid molecule lattice dynamics formalism should be applicable for these modes in *sym*-$C_6F_3Cl_3$. The experimental dispersion curves shown in Fig. 3 are compared with those calculated using the model of Chaplot[15] discussed in Sec. II and shown in Fig. 4. The agreement between the observed and calculated frequencies is generally very good, with the overall shapes of the branches agreeing well with observation for all these directions. The acoustic branches show good agreement, but there are more evident discrepancies for the optical branches, particularly at the zone boundaries. The largest discrepancy occurs for the highest frequency branch along **a***, where the calculated frequency is $\approx 8\%$ greater than that observed. However, for these highest frequency modes the rigid-molecule approximation will be less valid and the modes may interact with the lowest frequency internal vibrations. The result is expected to be a depression of the lattice mode frequencies relative to those of a "true" rigid molecule. The discrepancy between the observed and calculated frequencies for these modes may thus be due, at least partially, to these interactions. A further point of disagreement, which is not really highlighted in the figures, is that in the regions where there are several modes that are close in frequency the eigenvectors are not always correctly reproduced by the model. This is a common problem in lattice dynamics calculations, arising due to interactions between modes of the same symmetry and a similar frequency. It does not necessarily represent a significant failure of the essential model.

The parameters of the Chaplot model (Table I) show significant differences from those developed by Williams *et*

TABLE IV. Calculated elastic constants of $C_6F_3Cl_3$ at 5 K. Units are 10^9 N m^{-2}.

C_{11}	19.9 ± 2.1
C_{33}	13.5 ± 1.3
C_{44}	2.7 ± 0.2
C_{66}	8.9 ± 1.2

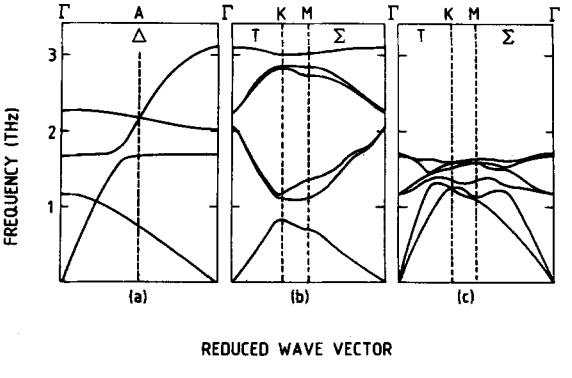

FIG. 4. Calculated phonon frequencies of $C_6F_3Cl_3$ using the model due to Chaplot (Ref. 15) described in the text. The separate diagrams directly correlate with those of Fig. 3.

TABLE V. Potential parameters of the Williams model (Ref. 7) used for phonon calculations. C(F) and C(Cl) are the carbon atoms bonded to the fluorine and chlorine atoms, respectively.[a]

Atom pair	A(kcal Å^6 mol^{-1})	B(kcal mol^{-1})	C(Å^{-1})
C(F)–C(F)	582.8	88 328	3.60
C(F)–C(Cl)	579.7	88 028	3.60
C(F)–F	355.7	92 310	3.88
C(F)–Cl	1038.1	139 683	3.555
C(Cl)–C(Cl)	576.6	87 730	3.60
C(Cl)–F	353.8	91 997	3.88
C(Cl)–Cl	1032.6	139 210	3.555
F–F	217.1	96 472	4.16
F–Cl	633.6	145 981	3.835
Cl–Cl	1847.1	220 897	3.51

[a] The atomic charges on atoms F, C(F), Cl, and C(Cl) were -0.174, 0.174, -0.109, and 0.109 electron units, respectively.

al.[7] Consequently, we have repeated the calculations using potential parameters of the Williams' form.[7] The heterointeractions F–Cl, which were not derived by Williams, were modeled by using the standard combining rules. The sets of Williams parameters developed so far also treat the carbon atoms slightly differently in the fluorine and chlorine potentials and so we used these different parameters for the two different carbon atoms in the *sym*-$C_6F_3Cl_3$ molecule. We incorporated electrostatic interactions by using a charged atom model, taking values of the charges from Williams.[7] Although this model gave qualitative agreement with the observed phonon frequencies, the quantitative agreement was significantly worse than for the Chaplot model.[15] In general, the Williams model overestimated the frequencies, usually by about 20% but in some cases by up to 40%. A summary of the potential model is given in Table V. The results for the calculated frequencies at the Γ point are given in Table VI. It is evident that the neutron and Raman data are in good agreement and are described much better by the Chaplot model than by the Williams model.

The crystal structure of *sym*-$C_6F_3Cl_3$ has only three parameters that are not determined by symmetry, namely two cell parameters and one molecular orientation parameter. Therefore, it is not possible to develop a full potential model for this system using static lattice modeling methods alone. The Chaplot model[15] already utilized dynamical frequencies to determine the potential parameters. The main information for the development of transferable potentials for C, F, Cl atoms will thus need to be obtained from other structures, and tested against the extensive lattice dynamics data presented in this paper. Attempts to use only the data reported here are unlikely to produce a model potential with the desired characteristic of transferability. Further work will need to explain why the Chaplot model is more successful than the transferable Williams model, which is a surprising result in view of the general success of the main Williams model. We anticipate that a general transferable set of C, F, Cl potential parameters that can successfully reproduce our dispersion curves for *sym*-$C_6F_3Cl_3$ will include electrostatic interactions in addition to the six-exponential terms.

V. CONCLUSION

We have presented an extensive set of measurements of the phonon dispersion curves in *sym*-$C_6F_3Cl_3$ at 5 K. At this temperature, harmonic lattice dynamics calculations within the rigid molecule approximation should be capable of reproducing most of the observed dispersion curves (with the possible exception of the highest frequency branches) and thus constitute a stringent test of any proposed intermolecular potentials. We have tested a model developed by Chaplot[15] that is based upon simple atom–atom six-exponential interactions, and have found that it does remarkably well in reproducing the observed frequencies. However, it is clear

TABLE VI. Phonon frequencies (in THz) at the Γ point calculated using the Williams model (Ref. 7) compared with Raman data, neutron data (Table II) and those calculated by the Chaplot model (Ref. 15).

	Experimental results				
	Raman		Neutron		
Mode	$T=11$ K	$T=295$ K	$T=5$ K	Williams model	Chaplot model
TDS	1.29	1.02	1.26 (2)	1.44	1.16
RZS	1.59	1.35	1.54 (3)	2.22	1.65
RZA			1.57 (3)	2.27	1.68
RDS	2.08	1.84	2.04 (4)	2.58	2.04
RDA			2.22 (3)	2.92	2.24
TZS			2.80 (3)	4.03	3.09

that there is still scope for improvement. We have shown that simple modifications to the transferable set of C, F, Cl parameters developed by Williams and co-workers[7] are unable to produce a model as good as the Chaplot model. We conclude therefore that either more work is necessary in order to develop a full set of transferable C, F, Cl potentials of the simple analytic form used here or a more elaborate description of the component terms of the total potential is required or the concept of transferability should be called in question.

ACKNOWLEDGMENTS

The project has received financial support from SERC (UK). One of the authors (M.T.D.) thanks the staff of Atomic Energy of Canada Limited for their kind hospitality during a number of visits to Chalk River. Another author (G.S.P.) thanks the staff of Risø for hospitality shown during a visit in which preliminary measurements were obtained.

[1]D. E. Williams and T. L. Starr, Comput. Chem. **1**, 173 (1977). A. Criado and R. Marquez, Acta Crystallogr. Sect. A **44**, 76 (1988).
[2]B. M. Powell, G. Dolling, and H. Bonadeo, J. Chem. Phys. **69**, 2428 (1978).
[3]X. Shi and L. S. Bartell, J. Phys. Chem. **92**, 5667 (1988).
[4]I. Natkaniec, E. L. Bokhenkov, B. Dorner, J. Kalus, G. A. Mackenzie, G. S. Pawley, U. Schmelzer, and E. F. Sheka, J. Phys. C. **13**, 4265 (1980).
[5]B. Dorner, E. L. Bokhenkov, S. E. Chaplot, J. Kalus, I. Natkaniec, G. S. Pawley, U. Schmelzer, and E. F. Sheka, J. Phys. C **15**, 2353 (1982).
[6]R. Righini, S. Califano, and S.M. Walmsley, Chem. Phys. **50**, 113 (1980).
[7]L. Y. Hsu and D. E. Williams, Acta. Crystallogr. Sect. A **36**, 277 (1980); D. E. Williams and S. R. Cox, Acta Crystallogr. Sect. B **40**, 404 (1984); D. E. Williams and L.Y. Hsu, Acta Crystallogr. Sect. A **41**, 296 (1985); D. E. Williams and D. J. Houpt, Acta Crystallogr. Sect. B **42**, 286 (1986).
[8]G. Dolling and B. M. Powell, Proc. R. Soc. London Ser. A **319**, 209 (1970); G. Dolling, G. S. Pawley, and B. M. Powell, Proc. R. Soc. London Ser. A **333**, 363 (1973); P. A. Reynolds, J. Chem. Phys. **59**, 2777 (1973); P. A. Reynolds, J. K. Kjems, and J. W. White, *ibid.* **60**, 824 (1974); S. L. Chaplot, A. Mierzejewski, G. S. Pawley, J. Lefebvre, and T. Luty. J. Phys. C **16**, 625 (1983).
[9]S. L. Chaplot, G. J. MacIntyre, A. Mierzejewski, and G. S. Pawley, Acta Crystallogr. Sect. B **37**, 1896 (1981).
[10]P. J. Wheatley, Acta Crystallogr. **8**, 224 (1955).
[11]J. H. Smith and A. I. M. Rae, J. Phys. C **11**, 1761 (1978).
[12]G. S. Pawley, Phys. Status Solidi B **49**, 475 (1972)
[13]J. H. S. Green and D. J Harrison, J. Mol. Spectrosc. **62**, 228 (1976).
[14]G. S. Pawley and S. J. Cyvin, J. Chem. Phys. **52**, 4073 (1970).
[15]S. L. Chaplot, Solid State Phys. (India) C **29**, 120 (1986).
[16]G. Dolling, B. M. Powell, B. H. Torrie, and G. S. Pawley, Can. J. Phys. **59**, 122 (1981).